Research Article

Title: Spatial transcriptomics reveals unique molecular fingerprints of human nociceptors

Authors: Diana Tavares-Ferreira[1,†], Stephanie Shiers[1,†], Pradipta R. Ray[1], Andi Wangzhou[1], Vivekanand Jeevakumar[1], Ishwarya Sankaranarayanan[1], Alexander Chamessian[2], Bryan A. Copits[2], Patrick M. Dougherty[3], Robert W. Gereau IV[2], Michael D. Burton[1], Gregory Dussor[1], Theodore J. Price[1,*]

Affiliations:
[1] University of Texas at Dallas, Department of Neuroscience and Center for Advanced Pain Studies
[2] Washington University at St. Louis, Department of Anesthesiology
[3] University of Texas MD Anderson Cancer Center, Department of Anesthesiology

[†]equally contributing first authors
[*]author for correspondence
Theodore J Price PhD
University of Texas at Dallas
800 W Campbell Rd
Richardson, TX 75080
972-883-4311
Theodore.price@utdallas.edu

One Sentence Summary (125 characters):

Three A-fiber mechanoreceptor and seven nociceptor subtypes are identified, revealing sex differences and unique aspects of human DRG neurons.

Abstract (125 words):

Single-cell transcriptomics on mouse nociceptors has transformed our understanding of pain mechanisms. Equivalent information from human nociceptors is lacking. We used spatial transcriptomics to molecularly characterize transcriptomes of single dorsal root ganglion (DRG) neurons from 8 organ donors. We identified 10 clusters of human sensory neurons, 6 of which are C nociceptors, 1 Aβ nociceptor, 1 Aδ, and 2 Aβ subtypes. These neuron subtypes have distinct expression profiles from rodents and non-human primates and we identify new markers for each of these subtypes that can be applied broadly in human studies. We also identify sex differences, including a marked increase in *CALCA* expression in female putative itch nociceptors. Our data open the door to new pain targets and unparalleled molecular characterization of clinical sensory disorders.

INTRODUCTION:

Pain is a major medical problem that has been treated for millennia with drugs whose origins can be traced to natural products.(*1*). While some new mechanism-based therapeutics have recently been approved for treatment of pain, these were developed based on biochemical observations in clinical studies, such as the calcitonin gene-related peptide (CGRP) link to migraine headache (*2*). There has been an unsatisfying failure to translate preclinical work on peripheral pain mechanisms, which has largely been done in rodents, into effective pain therapeutics (*3*). A potential explanation is that important species differences in nociceptor molecular phenotypes exist between mice and humans, an idea supported by bulk RNA sequencing experiments (*4, 5*), and other lines of evidence (*6, 7*).

Single cell sequencing of DRG neurons has delineated the molecular architecture of somatosensory neuron subtypes in the mouse (*8-10*), elucidated their developmental transcriptional paths (*11*) and characterized how these neurons change phenotype in response to injury (*12, 13*). This insight offers a molecular code for understanding the peripheral origins of different types of nociception, itch, thermal detection and touch in the mouse. However, it is not clear how this information can be applied to humans because a corresponding transcriptomic map of human somatosensory neurons does not exist. Most contemporary single cell profiling studies use nuclear RNA sequencing because this technology is scalable, fully commercialized and widely available. However, human DRG neurons are among the largest neurons in the body (20 – 100 µm diameter) (*14*) and also have large nuclei which create challenges for many sequencing platforms. To overcome these issues and fill this gap in knowledge we conducted spatial transcriptomic studies on human, lumbar dorsal root ganglia (DRG) obtained from organ donors. Because sex differences in pain mechanisms are increasing recognized, we performed our studies with an equal number of male and female samples.

RESULTS:

Spatial transcriptomics generates near single-neuron resolution

We generated whole cell transcriptomes for single neurons, using the 10X Genomics Visium Spatial Gene Expression platform (*15, 16*). This technology uses 55 µm barcoded-spots printed on the capture area of Visum slides (a total of 4,992 spots per capture area). Human DRGs, collected within 4 hrs of cross-clamp from neurologically dead organ donors (4 female and 4 male, details on organ donors provided in Table S1), were sectioned into the capture areas of the Visium slides, stained and imaged (**Fig 1A**). After tissue permeabilization, mRNA from each section was bound to barcoded primers and subsequently processed for library preparation and RNA sequencing. We obtained on average ~50M reads and detected an average total of ~24,000 genes per tissue section (**Fig S1A**). Because each tissue section was stained and imaged, the barcoded mRNAs and respective genes' location can be visualized within each DRG section using Loupe Browser (10x Genomics). In addition, barcoded spots can be selected based on their position on the tissue (**Fig S1B**). To generate near single-neuron resolution, we selected all barcodes that overlapped a single neuron in all sections and processed them for downstream analysis. From two 10 µm tissue sections from each of 8 donors, we identified a total of 4,356 barcodes that overlap a single neuron but also contained some adjacent cells (‘neuronal barcodes’) and 12,118 barcodes that directly surround neurons ('surrounding barcodes'). The remaining 20,725 barcoded spots were classified as 'other barcodes'. Barcodes that overlapped multiple neurons were excluded from downstream analysis. We optimized tissue permeabilization prior to sequencing to enhance neuronal RNA elution onto the slides to develop neuronally-enriched libraries. We detected a higher number of genes, and a higher number of mRNA molecules in the neuronal barcodes (**Fig S1C**). In addition, neuronal barcodes had a clear, distinct profile from surrounding and other barcodes (**Fig. S1D**).

Neuronal barcodes with a low number of reads and a low count for the neuronal marker *SNAP25* were removed, as described in methods. A total of 3,952 neuronal barcodes were grouped by donor ID and clustered using Seurat's anchor integration workflow

followed by graph-based clustering (*17*) (see Methods for detailed information and **Fig. S2**). We identified 10 clusters corresponding to low-threshold mechanoreceptors (LTMR) and nociceptors (**Fig. 1B**). For quality purposes, we verified the contribution of each sample for cluster formation (**Fig. 1C**) and the number of detected genes and unique molecules per cluster as well as the distribution of the neuronal marker *SNAP25* (**Fig. 1D**). We used several known neuronal markers from the literature to characterize the clusters based on their specific gene enrichment (**Fig. 1E**).

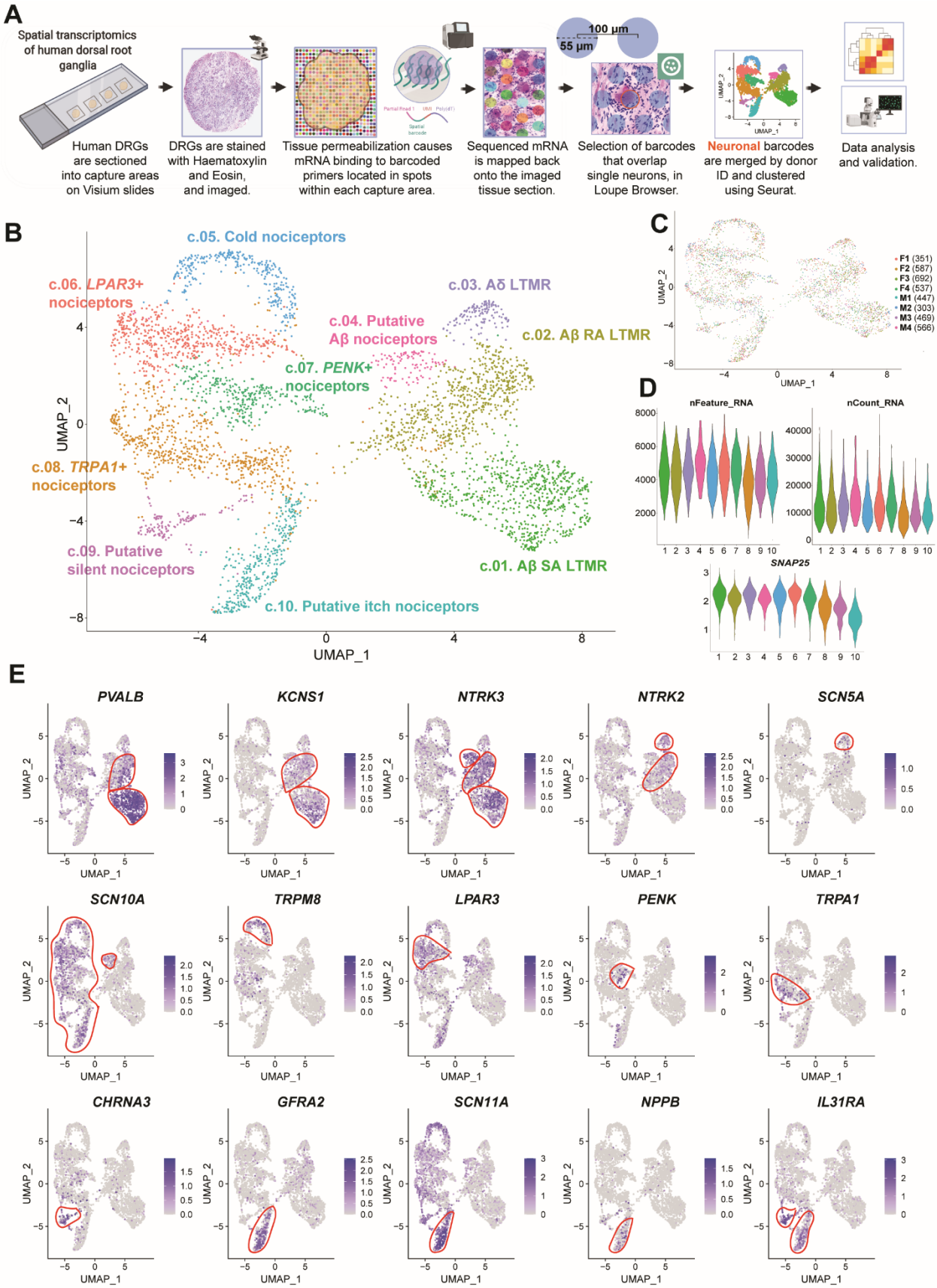
A
Spatial transcriptomics of human dorsal root ganglia
Human DRGs are sectioned into capture areas on Visium slides
DRGs are stained with Haematoxylin and Eosin, and imaged.
Tissue permeabilization causes mRNA binding to barcoded primers located in spots within each capture area.
Sequenced mRNA is mapped back onto the imaged tissue section.
100 µm
55 µm
Selection of barcodes that overlap single neurons, in Loupe Browser.
Neuronal barcodes are merged by donor ID and clustered using Seurat.
Data analysis and validation.
B
c.05. Cold nociceptors
c.06. LPAR3+ nociceptors
c.03. Aδ LTMR
c.04. Putative Aβ nociceptors
c.02. Aβ RA LTMR
c.07. PENK+ nociceptors
c.08. TRPA1+ nociceptors
c.09. Putative silent nociceptors
c.01. Aβ SA LTMR
c.10. Putative itch nociceptors
UMAP_1
UMAP_2
C
F1 (351)
F2 (587)
F3 (692)
F4 (537)
M1 (447)
M2 (303)
M3 (469)
M4 (566)
D
nFeature_RNA
nCount_RNA
SNAP25
E
PVALB
KCNS1
NTRK3
NTRK2
SCN5A
SCN10A
TRPM8
LPAR3
PENK
TRPA1
CHRNA3
GFRA2
SCN11A
NPPB
IL31RA

Figure 1: Identification of neuronal subtypes in human DRG using spatial transcriptomics. (A) Overview of the workflow and analysis. Barcoded spots on the Visium slides are 55 µm in diameter. **(B)** UMAP plot showing the labeled human DRG neuronal clusters. Neuronal barcodes (barcoded spots that overlap single neurons) were manually selected in Loupe Browser and clustered using Seurat package in R. **(C)** UMAP plot shows the contribution of each donor for cluster formation. The number of barcodes per sample used for clustering are in parenthesis. **(D)** Violin plots show consistent distributions of the number of detected genes (nFeature_RNA), the total counts of unique RNA molecules (nCount_RNA), and the counts for the neuronal marker *SNAP25* across clusters. The numbers on the x-axis correspond to cluster numbers: 1: Aβ SA LTMR, 2: Aβ RA LTMR, 3: Aδ LTMR, 4: Putative Aβ nociceptors, 5: Cold nociceptors, 6: *LPAR3*+ nociceptors, 7: *PENK*+ nociceptors, 8: *TRPA1*+ nociceptors, 9: Silent nociceptors, 10: Itch nociceptors. **(E)** UMAP plots of the expression of gene markers that were used to label neuronal clusters.

Defining human sensory neuron subtypes

DRG neurons are derived from neural crest cells and are responsible for transmitting all somatosensation (touch, proprioception, nociception and temperature) from the body to the brain (*18*). These neurons have been grouped into two main classes based on the diameter of the cell body and the conduction velocity. Myelinated Aβ neurons are large diameter cells that innervate the skin and detect non-noxious stimuli such as touch. They also innervate muscle and other structures to mediate proprioception. Unmyelinated, small diameter C-fiber neurons are critical for the detection of most noxious stimuli. A*∂* neurons are lightly myelinated and larger diameter than C fibers and respond to stimuli in the noxious range. These classes of sensory neurons differentially express specific neurotrophic receptors during development, and into adulthood (*18*). Within the A-fiber group, we identify four distinct subtypes. Cluster 1 was enriched in *NTRK3* and depleted from *NTRK2* a pattern of expression consistent with Aβ slowly-adapting (SA) LTMRs in the mouse (*19*). Aβ SA LTMRs innervate hairy and glabrous skin and terminate in Merkel cells (*20, 21*). A subset of these Aβ SA LTMRs also expressed *RUNX3* (**Fig. 2A**), which is a marker for proprioceptors in the mouse (*19*), suggesting that this group may also include proprioceptive Aβ neurons. The Aβ rapidly-adapting (RA) LTMR subgroup (cluster 2) was identified by expression of *NTRK3* and a low level of expression for *NTRK2 (19, 22)*. The end-organs of Aβ RA LTMRs are Meissner and Pacinian corpuscles in glabrous skin and lanceolate endings in hairy skin (*21*). Aδ-LTMR were characterized by their high level of expression of *NTRK2* and lack

of *NTRK3* (*19, 22*). Aδ-LTMR are also known as D-hair afferents and terminate as longitudinal lanceolate endings in hair follicles (*21*). Mice lacking this subset of *Ntrk2* positive neurons are less sensitive to touch and non-responsive to mechanical stimulation after injury (*23*). This suggests that Aδ fibers may be involved in the development of mechanical allodynia. The final group of A fiber neurons we identified expressed both *NTRK3* and *SCN10A*, a marker of nociceptive neurons, and therefore was identified as a putative Aβ-nociceptor subset. Aβ-fibers that respond to noxious stimuli have been reported in other species (*24*) including monkeys (*25*).

We identified six subtypes of C-fiber nociceptors (**Fig. 2A**). *TRPM8*, a known menthol and cold sensitive channel, labeled the cold nociceptors (cluster 5) (*26*). This cluster expresses *SCN10A* but little *TRPV1,* a unique feature compared to other nociceptor clusters. Cluster 6 was enriched for *LPAR3*, a receptor for Lysophosphatidic Acid (LPA). *LPAR3* labels a specific neuronal population in mouse DRG (*8*) and LPA and its receptors have been implicated in the development of neuropathic pain in mice (*27*). Higher levels of LPA are also associated with higher pain scores in human subjects that have neuropathic pain (*28*), suggesting an important role for this subpopulation in neuropathic pain. Proenkephalin (*PENK)* was enriched in cluster 7. *PENK* is an endogenous opioid and precursor to several enkephalins (*29*). Cluster 8 was labeled based on the expression of *TRPA1*. This neuronal sub-population also shows very high expression for *TAC1* (substance P) and *CALCA (30)* even though these neuropeptides were broadly expressed by all nociceptor clusters. This difference in neuropeptide expression is an important distinction between human and rodent sensory neurons, demonstrating peptidergic and non-peptidergic subsets of sensory neurons do not exist in humans. The specific expression of *CHRNA3* in cluster 9 identifies this group as putative 'silent' nociceptors (*31*). 'Silent' nociceptors correspond to a subset of C-fibers that innervate joints, viscera and skin. They are unresponsive to noxious stimuli under normal conditions, but become sensitized after inflammatory stimulation and likely play key roles in certain persistent pain disorders (*31, 32*). The itch nociceptor cluster was classified based on the expression of *NPPB*, *GFRA2* and *IL31RA (33).* Our data also shows that *SCN11A* is highly expressed in the putative itch sub-population. Itch and

pain are two different sensations. Nav1.9 (*SCN11A*) gain of function mutations have been described to lead to congenital insensitivity to pain (CIP) or partial loss of pain sensation. Studies in mice have reported that the mutation causes a pruritic phenotype (23, 24). Humans with Nav1.9 mutations report a severe pruritis (23, 25). Mechanisms associated with the very high expression of *SCN11A* in itch nociceptors may explain this phenotype. A distribution of genes associated with pain across human DRG neuronal subtype clusters is shown in **Fig. 2B**. Ranked gene expression by gene for all 10 neuronal barcode clusters are shown in **File S1**.

We labeled cluster 10 as putative itch nociceptors, but we speculate that it may also contain neuronal barcodes corresponding to C-LTMRs (**Fig S3A**). Upon initial analysis, this cluster was divided, but we merged it because we did not identify markers to distinguish the two sub-clusters. However, we note that *NPPB*, a classic marker for itch nociceptors, is expressed mainly in “pure” itch nociceptors (**Fig. S3B**). On the other hand, *GFRA2*, a characteristic marker of C-LTMRs in mice (*8*), was expressed in both sub-clusters. Itch and C-LTMR neurons both innervate outermost layers of skin, potentially explaining the transcriptional similarity within this cluster.

Spatial visualization of neuronal subtypes

Lumbar DRG neuronal subtypes did not show any clear spatial organization (**Fig. 2C**). We used visualization of barcode position of representative DRG sections to measure neuron diameter associated with each of the 10 clusters (see Methods). This validates that our Aβ clusters correspond to the largest diameter neurons in the DRG while C-nociceptors clusters were the smallest (**Fig. 2C; Fig. S4**), in line with cell size distributions in all other species where this has been assessed.

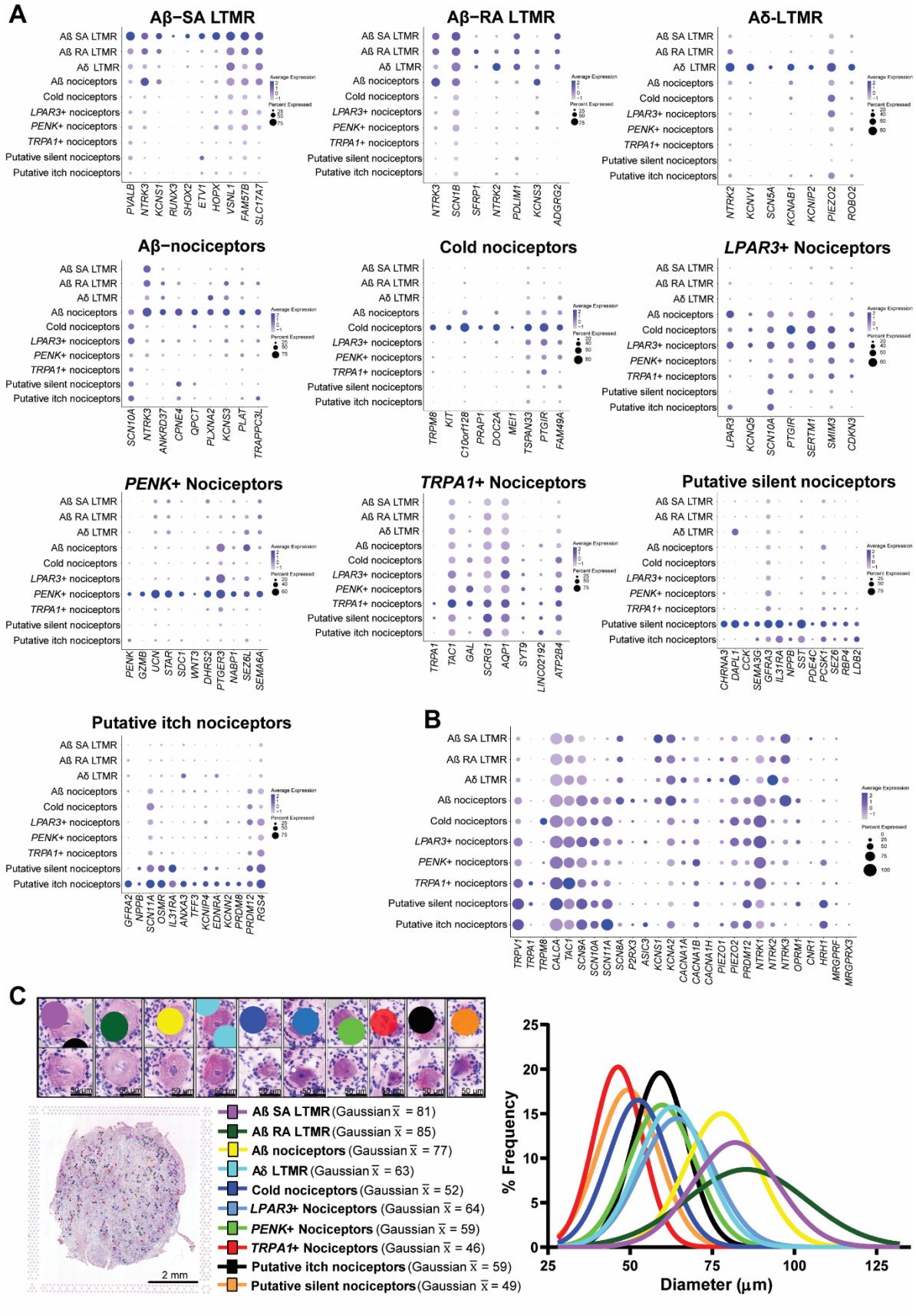
A
Aβ−SA LTMR
Aβ−RA LTMR
Aδ-LTMR
Aβ−nociceptors
Cold nociceptors
LPAR3+ Nociceptors
PENK+ Nociceptors
TRPA1+ Nociceptors
Putative silent nociceptors
Putative itch nociceptors
Aß SA LTMR
Aß RA LTMR
Aδ LTMR
Aß nociceptors
Cold nociceptors
LPAR3+ nociceptors
PENK+ nociceptors
TRPA1+ nociceptors
Putative silent nociceptors
Putative itch nociceptors
PVALB NTRK3 KCNS1 RUNX3 SHOX2 ETV1 HOPX VSNL1 FAM57B SLC17A7
NTRK3 SCN1B SFRP1 NTRK2 PDLIM1 KCNS3 ADGRG2
NTRK2 KCNV1 SCN5A KCNAB1 KCNIP2 PIEZO2 ROBO2
SCN10A NTRK3 ANKRD37 CPNE4 QPCT PLXNA2 KCNS3 PLAT TRAPPC3L
TRPM8 KIT C10orf128 PRAP1 DOC2A MEI1 TSPAN33 PTGIR FAM49A
LPAR3 KCNQ5 SCN10A PTGIR SERTM1 SMIM3 CDKN3
PENK GZMB UCN STAR SDC1 WNT3 DHRS2 PTGER3 NABP1 SEZ6L SEMA6A
TRPA1 TAC1 GAL SCRG1 AQP1 SYT9 LINC02192 ATP2B4
CHRNA3 DAPL1 CCK SEMA3G GFRA3 IL31RA NPPB SST PDE4C PCSK1 SEZ6 RBP4 LDB2
GFRA2 NPPB SCN11A OSMR IL31RA ANXA3 TFF3 KCNIP4 EDNRA KCNN2 PRDM8 PRDM12 RGS4
B
TRPV1 TRPA1 TRPM8 CALCA TAC1 SCN9A SCN10A SCN11A SCN8A P2RX3 ASIC3 KCNS1 KCNA2 CACNA1A CACNA1B CACNA1H PIEZO1 PIEZO2 PRDM12 NTRK1 NTRK2 NTRK3 OPRM1 CNR1 HRH1 MRGPRF MRGPRX3
C
50 µm
2 mm
Aß SA LTMR (Gaussian x̄ = 81)
Aß RA LTMR (Gaussian x̄ = 85)
Aß nociceptors (Gaussian x̄ = 77)
Aδ LTMR (Gaussian x̄ = 63)
Cold nociceptors (Gaussian x̄ = 52)
LPAR3+ Nociceptors (Gaussian x̄ = 64)
PENK+ Nociceptors (Gaussian x̄ = 59)
TRPA1+ Nociceptors (Gaussian x̄ = 46)
Putative itch nociceptors (Gaussian x̄ = 59)
Putative silent nociceptors (Gaussian x̄ = 49)
% Frequency
Diameter (µm)
0
5
10
15
20
25
50
75
100
125

Figure 2: Enriched gene expression in human DRG neuronal clusters and spatial visualization of neuronal subtypes. The size of the dot represents the percentage of barcodes within a cluster and the color corresponds to the average expression (scaled data) across all barcodes within a cluster (blue is high) for each gene shown. **(A)** Dot-plot showing the top genes for each neuronal sub-population and how they are expressed across all clusters. **(B)** Dot-plot showing the expression of known pain genes and markers across clusters. **(C)** Neuronal clusters were mapped back to three DRG sections to visualize neuronal cluster organization within the DRG. Diameters of neurons were measured to ascertain and plot cell sizes for each cluster with mean diameter (in μm). Gaussian curve fits are shown for visualization purposes.

Validation of spatial transcriptome-defined subtypes with RNAscope

Our spatial transcriptomic approach provides detailed insight into the types of neurons present in the human DRG, including their gene expression profiles, spatial location and size. However, the spatial sequencing approach we have employed has shortcomings, such as the lack of pure single cell transcriptomes for any given barcode. We have previously demonstrated that RNAscope *in situ* hybridization technology offers highly sensitive detection of neuronal mRNAs in human DRG (*7*). As a validation tool, we conducted RNAscope experiments on human DRG tissue sections for several mRNAs that showed high abundance in specific neuronal clusters: *PRDM12, NPPB*, *SST, NTRK1-3*. We assessed their co-expression with nociceptor-enriched genes *SCN10A*, *TRPV1*, and *CALCA* (**Fig. 3A**). The nociceptor population (*SCN10A*+, *TRPV1*+, or *CALCA+)* comprised ~60-70% of all human sensory neurons and were small in diameter (average = 54μm) (**Fig. 3B-C**). *PRDM12,* a gene that is essential for human pain perception (*34*) was expressed in ~74% of DRG neurons and co-expressed *CALCA* (**Fig. 3D**). *CALCA* mRNA was detected in all neuronal clusters and surrounding/other barcodes in the Visium platform, likely because *CALCA* mRNA localizes to axons (*35*) explaining its wide-spread detection. Smaller subdivisions of nociceptors such as the putative silent and itch nociceptor populations (*NPPB*+ or *SST*+) amounted to ~30% of the population and co-expressed *SCN10A* (**Fig. 3E-F**). *NTRK1,* which is most abundant in the nociceptor clusters, was found in 68% of the neuronal population and co-localized with *SCN10A* (**Fig. 3G**). *NTRK2* which was enriched in the Aδ LTMR cluster, a cluster that is depleted of *SCN10A,* was detected in medium sized neurons (**Fig. 3C**) and showed little co-expression with *SCN10A* (**Fig.**

3H). The Aβ-LTMR and Aβ-nociceptor marker, *NTRK3*, was found in larger sized neurons and showed slightly higher co-expression with *SCN10A* than *NTRK2*; most likely due its presence in the *SCN10A*+ Aβ-nociceptor cluster (**Fig. 3I**).

We have previously reported that *TRPV1* mRNA is more widely expressed in human nociceptors than in mouse (7) and *TRPV1* was detected in all nociceptor clusters with Visium, with the exception of cold nociceptors where it was expressed at very low levels. Using *SCN10A* as a nociceptor marker, we again observed that *TRPV1* was found in most nociceptors (**Fig 3J**). We next determined if these neurons were functionally responsive to the TrpV1 ligand, capsaicin. Application of capsaicin depolarized all small-sized, cultured human DRG neurons and caused action potential firing in 75% (**Fig 3K**). We conclude that RNAscope, spatial sequencing and functional analysis supports broad expression of TrpV1 in human nociceptors. As a final validation, previously published RNAscope findings substantiate the proposed neuronal subclusters from Visium sequencing (**Fig 3L**)(*7*). For example, we proposed *KCNS1* as a marker of human Aβ neurons due to its expression in large-sized neurons that were negative for *CALCA* and *P2RX3* (*7*). *KCNS1* was also enriched in Aβ clusters using the spatial transcriptomic approach.

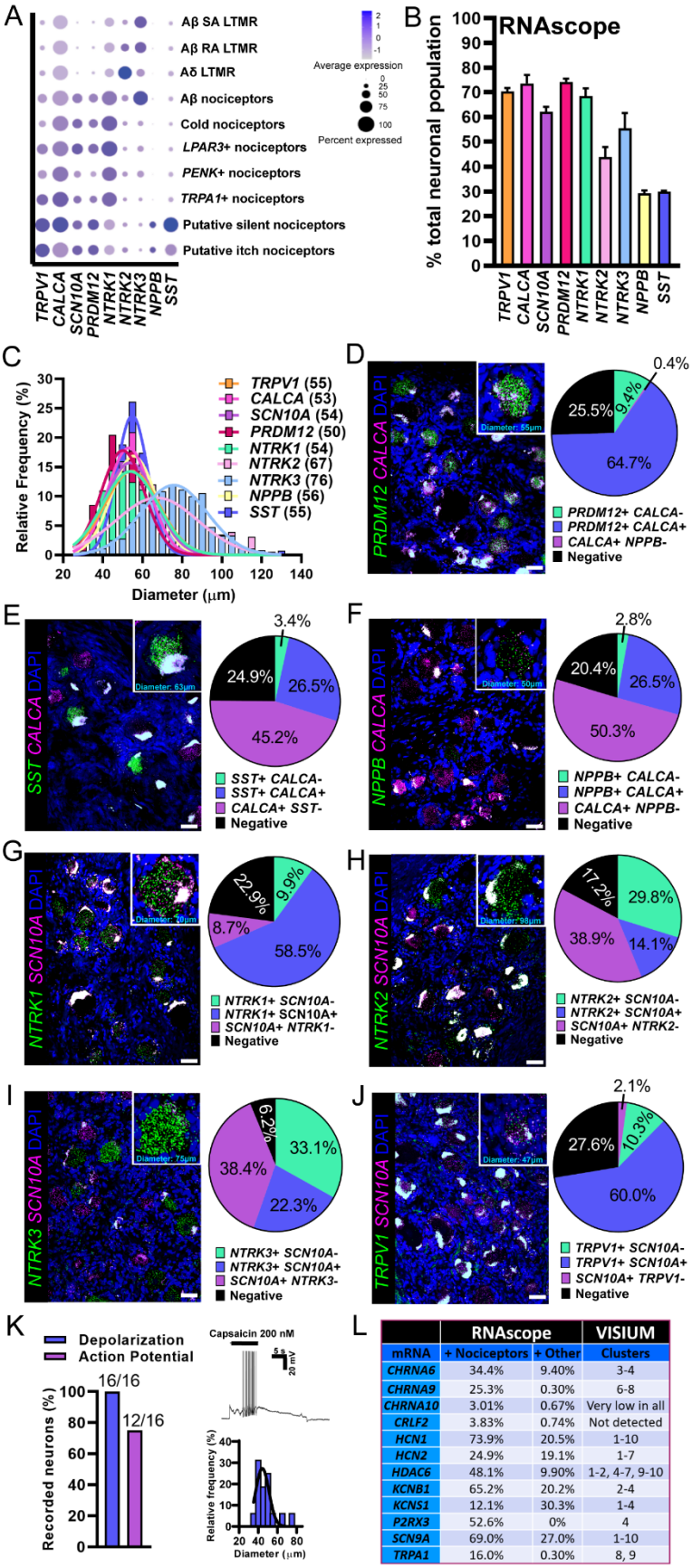

	RNAscope		VISIUM
mRNA	+ Nociceptors	+ Other	Clusters
CHRNA6	34.4%	9.40%	3-4
CHRNA9	25.3%	0.30%	6-8
CHRNA10	3.01%	0.67%	Very low in all
CRLF2	3.83%	0.74%	Not detected
HCN1	73.9%	20.5%	1-10
HCN2	24.9%	19.1%	1-7
HDAC6	48.1%	9.90%	1-2, 4-7, 9-10
KCNB1	65.2%	20.2%	2-4
KCNS1	12.1%	30.3%	1-4
P2RX3	52.6%	0%	4
SCN9A	69.0%	27.0%	1-10
TRPA1	16.0%	0.30%	8, 9

Fig. 3. RNAscope *in situ* hybridization and functional validation on human DRG. (A) Visualization of Visium gene expression for markers that were used for RNAscope analysis. **(B)** The percentage of neurons expressing each target compared to the total neuronal population. **(C)** The size distribution of all target-positive neurons. Gaussian mean in μm diameter in parentheses. **(D-J)** Merged image for the target of interest (green) with a known nociceptor marker (magenta) and DAPI (blue) is shown (scale bar = 50 μm). Inset for each panel shows a blow up of a single neuron. Population distribution of each neuronal marker is shown in the pie chart. **(K)** The TRPV1 agonist, capsaicin (200 nM), was applied to small diameter human DRG neurons *in vitro* causing depolarization (100%) and action potential firing (75%). **(L)** RNAscope data is summarized from (7) and compared to findings from Visium sequencing. The neuronal cluster for each target is listed. Clusters - 1: Aβ SA LTMR, 2: Aβ RA LTMR, 3: Aδ LTMR, 4: Aβ nociceptors, 5: Cold nociceptors, 6: *LPAR3+* nociceptors, 7: *PENK+* nociceptors, 8: *TRPA1+* nociceptors, 9: Silent nociceptors, 10: Itch nociceptors.

Sex differences in human sensory neurons

Molecular differences between male and female sensory neurons have been reported in defined population cell sequencing experiments in rodents (*36*) and inferred from bulk RNA-seq on human DRGs (*37*). We sought to determine sex differences in neuronal populations in the human DRG. We did not detect differences between males and females in DRG neuronal subtypes, because neurons from both sexes were clearly represented in all clusters (**Fig. 4A**). We then looked for sex differences with the overall population of neuronal barcodes, and within each cluster of specific sensory neuron types. With the Visium approach, neuronal barcodes include mRNA from surrounding cells. To overcome detection of generic sex differences contributed by other cell types, we performed statistical tests on surrounding barcodes (overall surrounding barcodes and surrounding barcodes specific to each neuronal cluster). We considered genes to be differentially expressed (DE) in neurons if they were not DE in the respective surrounding barcodes (**Fig. S5**). Similar to findings in the mouse where sex differences in the neuronal population were small (*36*), we identified only 44 genes with sex-differential expression in the neuronal barcodes pooled together but separated by sex (**Fig. 4B** and **File S2**). We then looked at potential sex-differences in each neuronal subtype. Here we found more neuronally-enriched DE genes, in specific nociceptor subtypes (**Fig. 4C**, **Files S3-S12 for neuronal barcodes, Files S13-23 for surrounding barcodes**). The itch population had the highest number of DE genes (82), suggesting molecular differences in mechanisms of pruritis between men and women. We performed gene-set enrichment analysis for DE genes in the itch population using GO (Gene Ontology) Enrichment Analysis resource, PANTHER (*38*). Most of the genes identified were involved in cell communication and signaling and regulation of MAPK cascade (**File S24**). A striking difference was the increase in *CALCA* found in female itch nociceptors (**Fig 4D**). This finding was validated in RNAscope experiments examining *CALCA* expression in *NPPB*-positive neurons from male and female organ donors (**Fig. 4E; Fig. S6**).

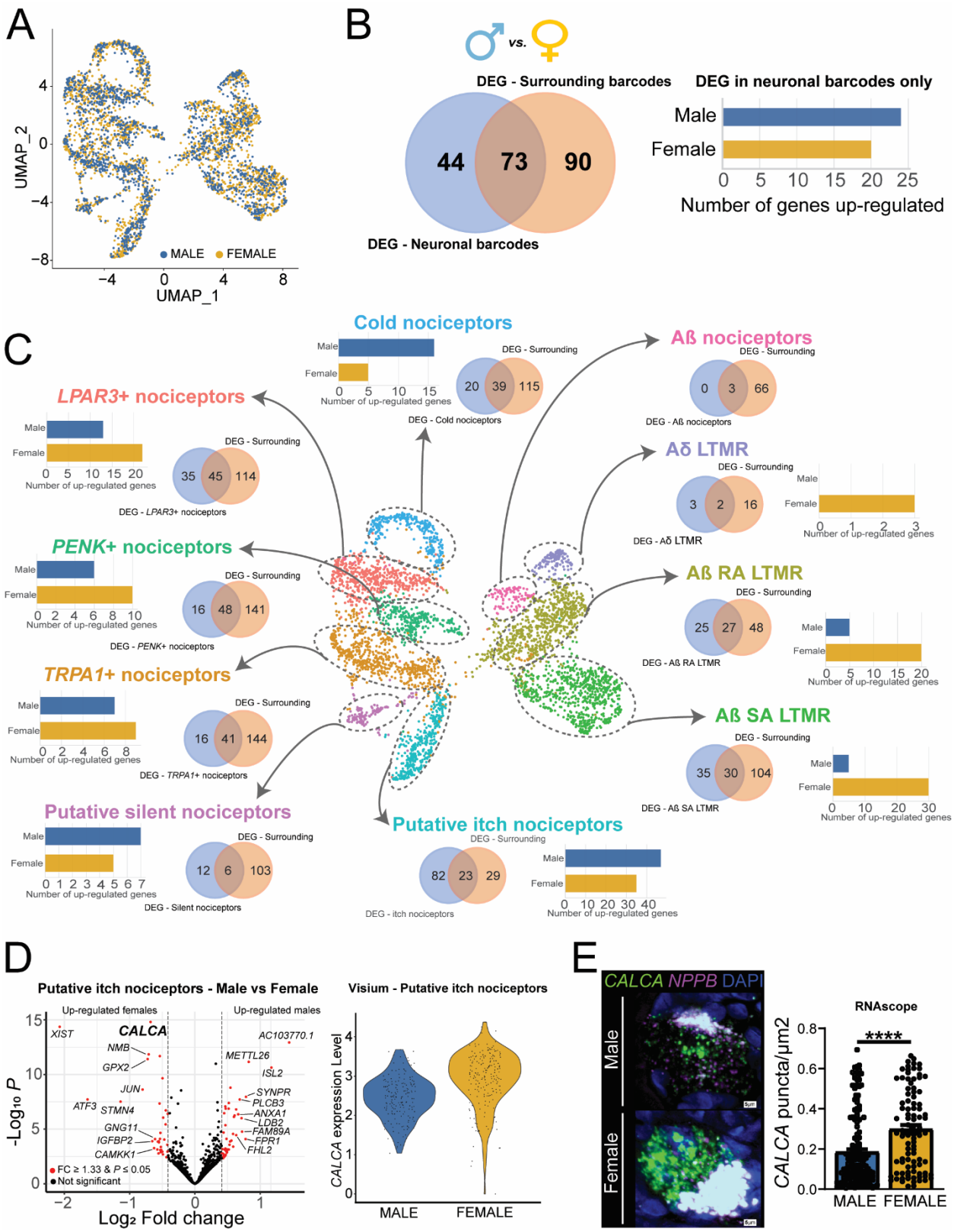

Fig. 4. Sex-differences in gene expression within human DRG neuronal populations. (A) UMAP showing that males and female samples are equally represented in all clusters. **(B)** Venn diagram showing the overlap between the number of DE genes

in the overall neuronal population and the overall surrounding population of barcodes. Bar-plot showing the number of up-regulated genes per sex after removing genes that were also DE in surrounding barcodes. **(C)** Venn diagrams show the overlap between the number of DE genes in each neuronal subtype and the respective surrounding population. Bar-plots show the number of up-regulated genes per sex in each cluster after removing genes that were also DE in the respective surrounding barcodes. **(D)** Volcano plot shows DE genes in the itch population after removing DE genes in surrounding barcodes (we highlighted the top 10 genes in each sex ranked by $\log_2$ fold change). Violin plot shows *CALCA* expression in individual barcodes in males and female within the itch population. **(E)** RNAscope for *CALCA* mRNA colocalized with *NPPB*, a marker of itch nociceptors, with quantification of differences in expression between male and female neurons for amount of *CALCA* expression in the dot-plot. Representative image scale bar = 5 μm. DE = differentially expressed.

DISCUSSION:

Our work demonstrates that Visium spatial transcriptomics can be used to generate near-single neuron resolution to define, for the first time, molecular profiles of neuronal subtypes in the human DRG. Our findings demonstrate substantial differences between mouse, where most single nociceptor transcriptome work has been done, and human nociceptors. One area where this evolutionary divergence between mouse and human sensory neurons is striking is in neuropeptide, *TRPV1* and *NTRK1* expression. Most human nociceptors share expression of these genes suggesting a blending of many of the markers of peptidergic and non-peptidergic nociceptors that are found in other species, in particular the mouse. Another striking difference is the *TRPM8* population. In the mouse, *Trpm8*-positive cells make up three sub-clusters that express several gene markers that are not found in this population in humans (*10*). Additionally, human *TRPM8*-positive express *SCN10A* while mouse *Trpm8* neurons do not. We also found important differences in the putative itch nociceptor population with more widespread expression of many markers, in particular into the silent nociceptor subset of neurons. Finally, we do not find expression for most known markers of C-LTMRs in human DRG. This includes lack of markers that were recently identified in a nuclear sequencing study from Rhesus macaques (*39*). An exception may be *GFRA2* expression which we found marked a subset of putative itch nociceptors that we speculate may be C-LTMRs.

Our spatial transcriptomic characterization of human DRG neuronal subtypes should enable new discoveries in the pain and sensory neuroscience field. One important advance is the identification of sets of markers that can be used to molecularly phenotype subtypes of sensory neurons that can be sampled through skin biopsies and other methods from neuropathy patients. While there are clear indications of pathology in sensory neurons indicated from clinical skin biopsy studies, these are almost always grouped into small and large fiber neuropathies but further distinctions cannot be made. Our work enables greater mechanistic insight from routine clinical tests. The finding that neuronal transcriptomes in the DRG are stable unless frank axonal injury has occurred (*12*) suggests that our dataset can be utilized for this purpose almost immediately. Our dataset can also be used to mine for pharmacological targets that can be used to specifically manipulate the excitability of different subsets of nociceptors. This offers the possibility for development of better pain targets that are developed based entirely on human data, without reliance on animal models where conservation may not be clear. Our dataset is “sex-aware” insofar as it contains both male and female samples. We highlight some sex differences (e.g. greater CGRP expression in the itch nociceptor population in females) that may be important considerations for therapeutic development. Finally, this dataset can be a foundation to more thoroughly vet targets that have been discovered in studies of peripheral nerves in animal pain models. Our findings now make it possible for conservation of gene expression in human nociceptors to be a first step in de-risking pain targets for future drug development.

References and Notes:

1. J. Scholz, C. J. Woolf, Can we conquer pain? *Nat Neurosci* **5 Suppl**, 1062 (Nov, 2002).
2. L. Edvinsson, K. A. Haanes, K. Warfvinge, D. N. Krause, CGRP as the target of new migraine therapies - successful translation from bench to clinic. *Nat Rev Neurol* **14**, 338 (Jun, 2018).
3. J. S. Mogil, The translatability of pain across species. *Philos Trans R Soc Lond B Biol Sci* **374**, 20190286 (Nov 11, 2019).
4. P. Ray *et al.*, Comparative transcriptome profiling of the human and mouse dorsal root ganglia: an RNA-seq-based resource for pain and sensory neuroscience research. *Pain* **159**, 1325 (Jul, 2018).
5. A. Wangzhou *et al.*, Pharmacological target-focused transcriptomic analysis of native vs cultured human and mouse dorsal root ganglia. *Pain* **161**, 1497 (Jul, 2020).
6. S. J. Middleton *et al.*, Studying human nociceptors: from fundamentals to the clinic. *Brain* **in press**, (2021).
7. S. Shiers, R. M. Klein, T. J. Price, Quantitative differences in neuronal subpopulations between mouse and human dorsal root ganglia demonstrated with RNAscope in situ hybridization. *Pain* **161**, 2410 (Oct, 2020).
8. D. Usoskin *et al.*, Unbiased classification of sensory neuron types by large-scale single-cell RNA sequencing. *Nat Neurosci* **18**, 145 (Jan, 2015).
9. Y. Zheng *et al.*, Deep Sequencing of Somatosensory Neurons Reveals Molecular Determinants of Intrinsic Physiological Properties. *Neuron* **103**, 598 (Aug 21, 2019).
10. A. Zeisel *et al.*, Molecular Architecture of the Mouse Nervous System. *Cell* **174**, 999 (Aug 9, 2018).
11. N. Sharma *et al.*, The emergence of transcriptional identity in somatosensory neurons. *Nature* **577**, 392 (Jan, 2020).
12. W. Renthal *et al.*, Transcriptional Reprogramming of Distinct Peripheral Sensory Neuron Subtypes after Axonal Injury. *Neuron* **108**, 128 (Oct 14, 2020).
13. M. Q. Nguyen, C. E. Le Pichon, N. Ryba, Stereotyped transcriptomic transformation of somatosensory neurons in response to injury. *Elife* **8**, (Oct 8, 2019).
14. R. V. Haberberger, C. Barry, N. Dominguez, D. Matusica, Human dorsal root ganglia. *Frontiers in cellular neuroscience* **13**, 271 (2019).
15. P. L. Ståhl *et al.*, Visualization and analysis of gene expression in tissue sections by spatial transcriptomics. *Science* **353**, 78 (2016).
16. N. Rao, S. Clark, O. Habern, Bridging Genomics and Tissue Pathology: 10x Genomics explores new frontiers with the Visium Spatial Gene Expression Solution. *Genetic Engineering & Biotechnology News* **40**, 50 (2020).
17. T. Stuart *et al.*, Comprehensive integration of single-cell data. *Cell* **177**, 1888 (2019).
18. D. W. Raible, J. M. Ungos, in *Neural Crest Induction and Differentiation*. (Springer, 2006), pp. 170-180.
19. C. Peng *et al.*, Termination of cell-type specification gene programs by the miR-183 cluster determines the population sizes of low-threshold mechanosensitive neurons. *Development* **145**, (2018).

20. R. S. Johansson, A. Vallbo, Tactile sensibility in the human hand: relative and absolute densities of four types of mechanoreceptive units in glabrous skin. *The Journal of physiology* **286**, 283 (1979).
21. V. E. Abraira, D. D. Ginty, The sensory neurons of touch. *Neuron* **79**, 618 (2013).
22. W. Olson, P. Dong, M. Fleming, W. Luo, The specification and wiring of mammalian cutaneous low-threshold mechanoreceptors. *Wiley Interdisciplinary Reviews: Developmental Biology* **5**, 389 (2016).
23. R. Dhandapani *et al.*, Control of mechanical pain hypersensitivity in mice through ligand-targeted photoablation of TrkB-positive sensory neurons. *Nature communications* **9**, 1 (2018).
24. L. Djouhri, S. N. Lawson, Aβ-fiber nociceptive primary afferent neurons: a review of incidence and properties in relation to other afferent A-fiber neurons in mammals. *Brain Research Reviews* **46**, 131 (2004).
25. R.-D. Treede, R. A. Meyer, J. N. Campbell, Myelinated mechanically insensitive afferents from monkey hairy skin: heat-response properties. *Journal of neurophysiology* **80**, 1082 (1998).
26. D. D. McKemy, W. M. Neuhausser, D. Julius, Identification of a cold receptor reveals a general role for TRP channels in thermosensation. *Nature* **416**, 52 (2002).
27. H. Ueda, H. Matsunaga, O. I. Olaposi, J. Nagai, Lysophosphatidic acid: chemical signature of neuropathic pain. *Biochimica et Biophysica Acta (BBA)-Molecular and Cell Biology of Lipids* **1831**, 61 (2013).
28. K. Kuwajima *et al.*, Lysophosphatidic acid is associated with neuropathic pain intensity in humans: An exploratory study. *PloS one* **13**, e0207310 (2018).
29. R. Przewl·ocki, in *Hormones, brain and behavior*. (Elsevier, 2002), pp. 691-733.
30. R. Nassini, S. Materazzi, S. Benemei, P. Geppetti, in *Reviews of Physiology, Biochemistry and Pharmacology, Vol. 167*. (Springer, 2014), pp. 1-43.
31. V. Prato *et al.*, Functional and molecular characterization of mechanoinsensitive “silent” nociceptors. *Cell reports* **21**, 3102 (2017).
32. M. Michaelis, H. J. Häbler, W. Jaenig, Silent afferents: a separate class of primary afferents? *Clinical and experimental pharmacology and physiology* **23**, 99 (1996).
33. S. K. Mishra, M. A. Hoon, The cells and circuitry for itch responses in mice. *Science* **340**, 968 (May 24, 2013).
34. Y. C. Chen *et al.*, Transcriptional regulator PRDM12 is essential for human pain perception. *Nat Genet* **47**, 803 (Jul, 2015).
35. C. C. Toth *et al.*, Locally synthesized calcitonin gene-related Peptide has a critical role in peripheral nerve regeneration. *J Neuropathol Exp Neurol* **68**, 326 (Mar, 2009).
36. C. J. A. Smith-Anttila *et al.*, Identification of a Sacral, Visceral Sensory Transcriptome in Embryonic and Adult Mice. *eNeuro* **7**, (Jan/Feb, 2020).
37. P. Ray *et al.*, Comparative transcriptome profiling of the human and mouse dorsal root ganglia: an RNA-seq-based resource for pain and sensory neuroscience research. *Pain* **159**, 1325 (2018).
38. H. Mi, A. Muruganujan, D. Ebert, X. Huang, P. D. Thomas, PANTHER version 14: more genomes, a new PANTHER GO-slim and improvements in enrichment analysis tools. *Nucleic acids research* **47**, D419 (2019).

39. J. Kupari *et al.,* Single cell transcriptomics of primate sensory neurons identifies cell types associated with human chronic pain. *bioRxiv,* 2020.12.07.414193 (2020).

Acknowledgements: The authors thank the organ donors and their families for their enduring gift. We thank Anna Cervantes, Erin Vines and Dr. Jeffrey Reese at the Southwest Transplant Alliance for coordinating and procuring DRGs from organ donation surgeries. We also thank members of the Price Lab, Moeno Kume, Dr. Muhammad Saad Yousuf, Dr. Amelia Balmain, Juliet Mwirigi for assistance in DRG procurement. The authors acknowledge the Genome Center at The University of Texas at Dallas for their support during this course of research. **Funding:** This work was supported by NIH grants NS111929 to PMD and TJP, NS065926 to GD and TJP and NS042595 to RWG IV. **Author contributions:** DT-F and SS conducted Visium spatial optimization and gene expression protocol. DT-F performed all computational analyses. SS performed RNAscope and analysis. VJ performed electrophysiology. PRR and AW assisted in computational analyses. IS assisted in Visium experiments. AC and BC trained staff on DRG surgical extraction and established DRG procurement protocols. DT-F, SS and TJP wrote the manuscript. DT-F, SS, PRR, PMD, RWG IV, MDB, GD and TJP designed the study. PRR, GD and TJP supervised the study. PMD, RWG IV, GD and TJP obtained funding for the study. All authors read and edited the paper. **Competing interests:** PRR, AW, GD and TJP are founders of Doloromics. The authors declare no other conflicts of interest. **Data and materials availability:** Raw sequencing data will be deposited in the dbGaP repository. Public access to processed data is available at sensoryomics.com. All analyses scripts and loupe browser files are available upon request.

Ethics approval: This work was approved by the University of Texas at Dallas Institutional Review Board. Original approval date for protocol MR 15-237 - *The Human Dorsal Root Ganglion Transcriptome* was Sept 21, 2015. The protocol was renewed and has a current expiration date of Jan 22, 2023.

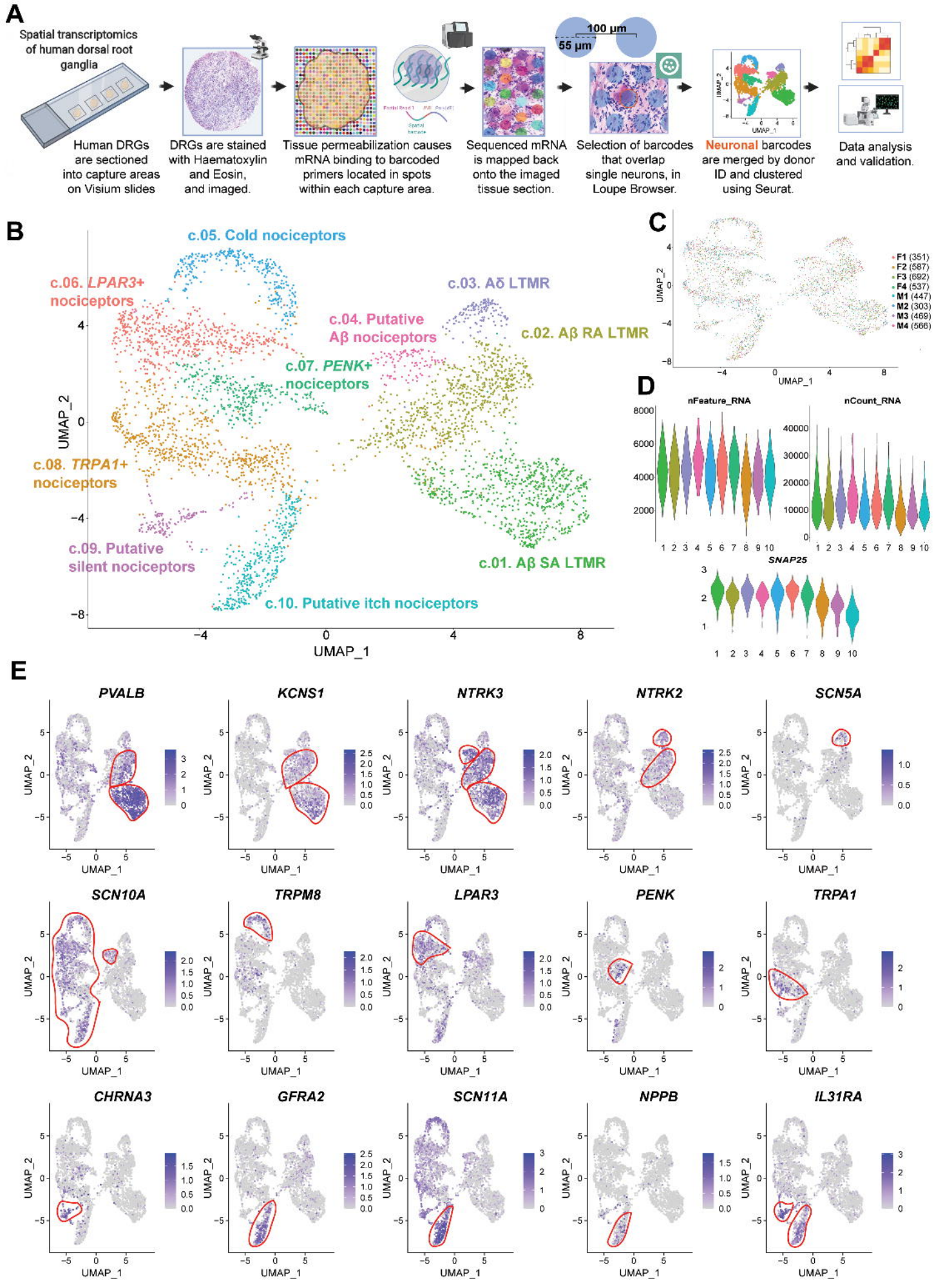
A
Spatial transcriptomics of human dorsal root ganglia
Human DRGs are sectioned into capture areas on Visium slides
DRGs are stained with Haematoxylin and Eosin, and imaged.
Tissue permeabilization causes mRNA binding to barcoded primers located in spots within each capture area.
Sequenced mRNA is mapped back onto the imaged tissue section.
100 µm
55 µm
Selection of barcodes that overlap single neurons, in Loupe Browser.
Neuronal barcodes are merged by donor ID and clustered using Seurat.
Data analysis and validation.
B
c.05. Cold nociceptors
c.06. LPAR3+ nociceptors
c.03. Aδ LTMR
c.04. Putative Aβ nociceptors
c.02. Aβ RA LTMR
c.07. PENK+ nociceptors
c.08. TRPA1+ nociceptors
c.09. Putative silent nociceptors
c.01. Aβ SA LTMR
c.10. Putative itch nociceptors
UMAP_1
UMAP_2
C
F1 (351)
F2 (587)
F3 (692)
F4 (537)
M1 (447)
M2 (303)
M3 (469)
M4 (566)
D
nFeature_RNA
nCount_RNA
SNAP25
E
PVALB
KCNS1
NTRK3
NTRK2
SCN5A
SCN10A
TRPM8
LPAR3
PENK
TRPA1
CHRNA3
GFRA2
SCN11A
NPPB
IL31RA

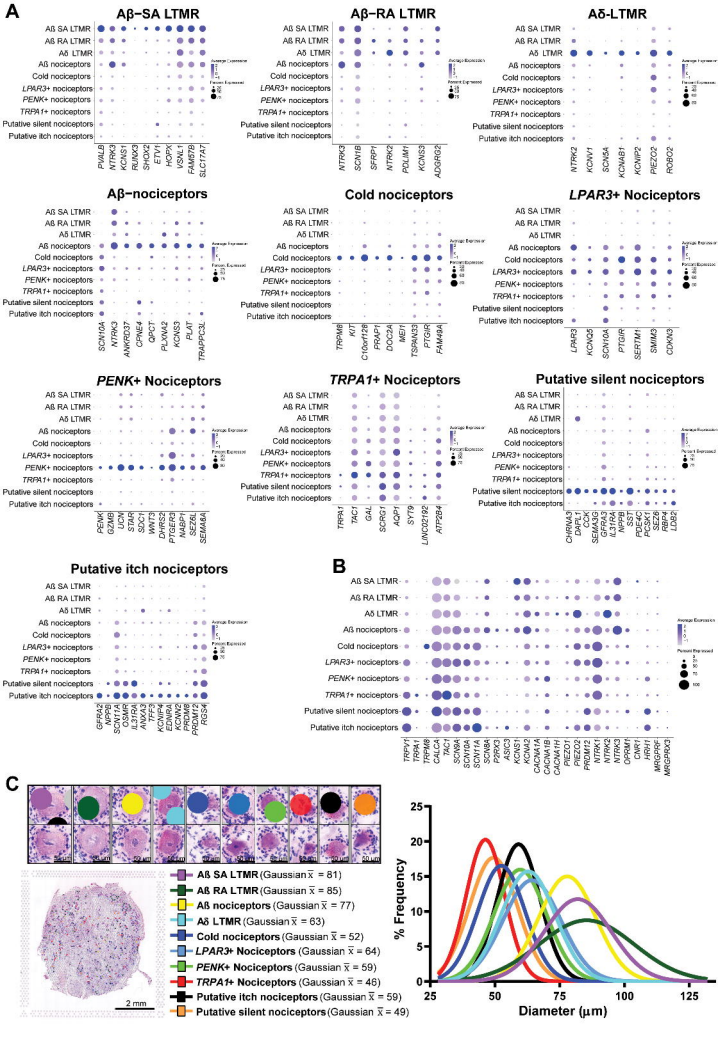
A
Aβ-SA LTMR
Aδ-RA LTMR
Aδ-LTMR
Aβ-nociceptors
Cold nociceptors
PENK+ Nociceptors
TRPA1+ Nociceptors
Putative silent nociceptors
Putative itch nociceptors
Aδ SA LTMR
Aδ RA LTMR
Aδ LTMR
Aβ nociceptors
Cold nociceptors
LPAR3+ nociceptors
PENK+ nociceptors
TRPA1+ nociceptors
Putative silent nociceptors
Putative itch nociceptors
PVALB
KCNS3
RUNX3
SHOX2
ETV1
HSX1
FAM57B
SLC17A7
NTRK3
SCN1B
SFRP1
NTRK2
PDLIM1
KCNS3
ADGRG2
NTRK2
KCNV1
SCN5A
KCNAB1
KCNIP2
PIEZO2
RORB2
SCN10A
NTRK3
AMPKA2
QPCT
PLXNA2
KCNS3
PLAT
TRAPPC3L
TRPM8
KIT
C1orf116
PRKCE
DDC2A
MEF
TSPAN13
PTGIR
FAM49A
LPAR3
KCNK25
SCN10A
PTGIR
SERTM1
SMIM3
CDKN3
PENK
GABRA2
UCN
STAR
SCC1
CCK4
DVR52
PTGER3
NPW
SERPI
SEMA6A
TRPA1
TAC1
GAL
SCRG1
AQP1
SYT9
LINC02192
ATP2B4
CHRNA3
DAPL1
CCK4
SEMA3G
CRTAC1
NPW
PDE4C
PCSK1
GPR151
RBP4
LDB2
GFRA3
NPW
SCN11A
CDH18
IL31RA
ANXA3
KIT
KCNIP4
PRDM8
KCNK20
PRDM8
PRKCE
RGS4
B
TRPV1
TRPA1
TRPM8
CALCA
TAC1
SCN9A
SCN10A
SCN11A
SCN1B
P2RX3
ASIC3
KCNG4
KCNA2
CACNA1A
CACNA1B
CACNA1H
PIEZO1
PIEZO2
PDE4D
NTRK1
NTRK2
NTRK3
OPRM1
CNR1
TRPV4
MRGPRD
MRGPRX3
C
Aδ SA LTMR
Aδ RA LTMR
Aδ LTMR
2 mm
Aδ SA LTMR (Gaussian x̄ = 81)
Aδ RA LTMR (Gaussian x̄ = 85)
Aδ nociceptors (Gaussian x̄ = 77)
Aδ LTMR (Gaussian x̄ = 63)
Cold nociceptors (Gaussian x̄ = 52)
LPAR3+ Nociceptors (Gaussian x̄ = 64)
PENK+ Nociceptors (Gaussian x̄ = 59)
TRPA1+ Nociceptors (Gaussian x̄ = 46)
Putative itch nociceptors (Gaussian x̄ = 59)
Putative silent nociceptors (Gaussian x̄ = 49)
% Frequency
Diameter (μm)

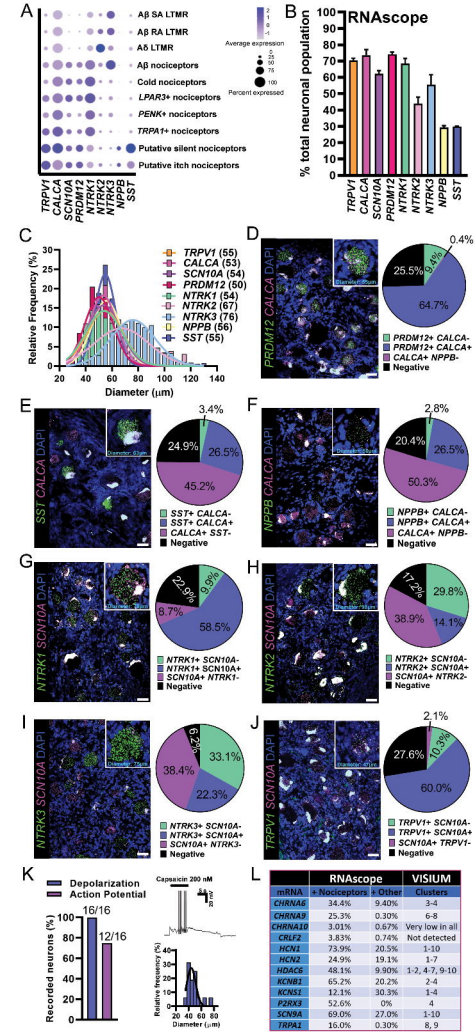

	RNAscope		VISIUM
mRNA	+ Nociceptors	+ Other	Clusters
CHRNA6	34.4%	9.40%	3-4
CHRNA9	25.3%	0.30%	6-8
CHRNA10	3.01%	0.67%	Very low in all
CRLF2	3.83%	0.74%	Not detected
HCN1	73.9%	20.5%	1-10
HCN2	24.9%	19.1%	1-7
HDAC6	48.1%	9.90%	1-2, 4-7, 9-10
KCNB1	65.2%	20.2%	2-4
KCNS1	12.1%	30.3%	1-4
P2RX3	52.6%	0%	4
SCN9A	69.0%	27.0%	1-10
TRPA1	16.0%	0.30%	8, 9

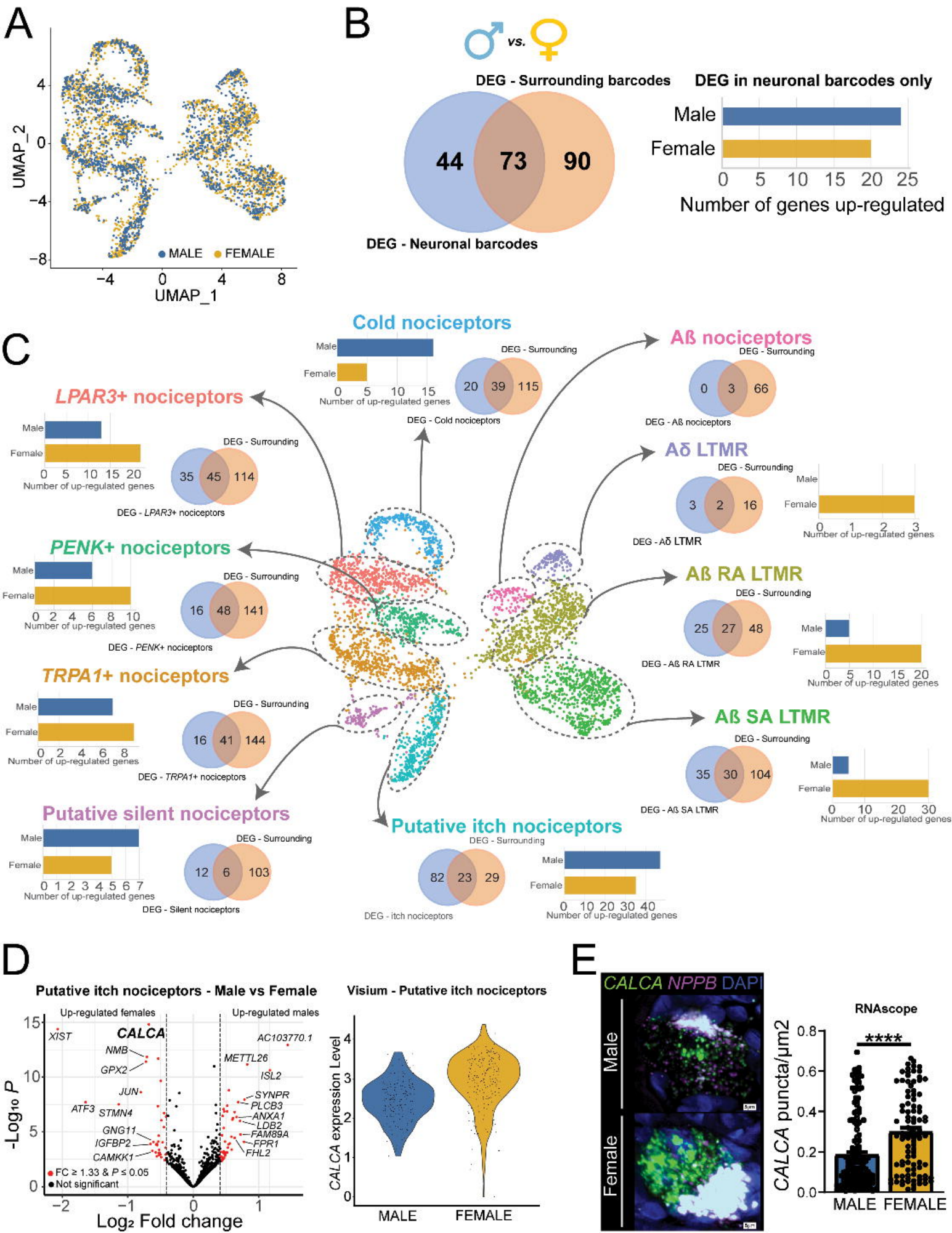
A
UMAP_2
UMAP_1
MALE
FEMALE
B
vs.
DEG - Surrounding barcodes
DEG - Neuronal barcodes
44
73
90
DEG in neuronal barcodes only
Male
Female
Number of genes up-regulated
C
Cold nociceptors
Male
Female
Number of up-regulated genes
DEG - Surrounding
20 39 115
DEG - Cold nociceptors
Aß nociceptors
0 3 66
DEG - Aß nociceptors
LPAR3+ nociceptors
35 45 114
DEG - LPAR3+ nociceptors
Aδ LTMR
3 2 16
DEG - Aδ LTMR
PENK+ nociceptors
16 48 141
DEG - PENK+ nociceptors
Aß RA LTMR
25 27 48
DEG - Aß RA LTMR
TRPA1+ nociceptors
16 41 144
DEG - TRPA1+ nociceptors
Aß SA LTMR
35 30 104
DEG - Aß SA LTMR
Putative silent nociceptors
12 6 103
DEG - Silent nociceptors
Putative itch nociceptors
82 23 29
DEG - itch nociceptors
D
Putative itch nociceptors - Male vs Female
Up-regulated females
Up-regulated males
XIST
CALCA
NMB
GPX2
JUN
ATF3
STMN4
GNG11
IGFBP2
CAMKK1
AC103770.1
METTL26
ISL2
SYNPR
PLCB3
ANXA1
LDB2
FAM89A
FPR1
FHL2
FC ≥ 1.33 & P ≤ 0.05
Not significant
-Log10 P
Log2 Fold change
Visium - Putative itch nociceptors
CALCA expression Level
MALE
FEMALE
E
CALCA NPPB DAPI
Male
Female
RNAscope
CALCA puncta/µm2
****
MALE
FEMALE